Proceedings of the Canadian Society for Mechanical Engineering International Congress 2022
CSME Congress 2022
June 5-8, 2022, Edmonton, AB, Canada

Towards a cicrcular process for additive manufacturing of fashion footwear

Chahine Ghimouz[1], Julie Tzeng[2], Jean Pierre Kenné[1], Lucas A. Hof[1*]
[1]Department of Mechanical Engineering, École de Technologie Supérieure, Montreal, Canada
[2]Arshae, Montreal, Canada

[*]lucas.hof@etsmtl.ca

Abstract — The global fashion industry is struggling with carbon footprint issues, but technological innovations are supporting to improve its performance and environmental efficiency in terms of footwear manufacturing. The Quebec-based footwear company Arshae aims to create a line of shoes that are fully 3D printed. The company's manufacturing approach is based on sustainability by designing models to facilitate disassembly in order to recycle each component of the shoe efficiently and feed them back in a closed loop manufacturing cycle. This paper focuses on providing technical solutions to the assembly system without chemical glue or thermal processes by proposing a mechanical snapfit to keep the assembly in place during the use of the shoe. An analytical calculation is performed to design an efficient snapfit and validate it through numerical finite element simulations. The results of this study contribute to the demonstration of 3D printing high-heeled shoes in order to facilitate their reinsertion into a closed "circular" manufacturing loop.

Keywords: circular manufacturing, additive manufacturing, 3D printing, polymer materials, Selective Laser Sintering, Multi Jet Fusion, snapfit design, assembly/disassembly, footwear

I. INTRODUCTION

In this twenty-first century, the global consumption of natural resources is constantly increasing. Currently, the quantities of natural resources consumed in the world annually are so excessive that natural resources are consumed at higher rate as needed to regenerate them by the planet according to the World Wildlife Fund foundation (WWF) [1]. In fact, at this moment it takes the planet 1.7 years to regenerate all the resources consumed in one year [2]. In 2010, 72 billion tons of raw materials were extracted and consumed, which is double compared to the amounts extracted in 1980, according to a report of the Organization for Economic Cooperation and Development published in 2015 [3]. With the current economic growth, annual consumption will reach the symbolic bar of 100 billion tons around 2030 [4].

Part of this acceleration in the consumption of raw materials is due to the economic system in which we have evolved over the last century, which consists of a linear model (Take, Make, Use and Dispose), also known as the "linear economy". In order to overcome this problem of over-consumption and the environmental catastrophe that the planet is going through, a more sustainable, "circular economy (CE)" model has been proposed. This new way of approaching the economy is claimed to be the state of mind of companies that will help move towards long-term sustainable development [5].

Arshae is a Canadian company that offers an end-to-end solution that considers the entire life cycle of footwear by building a closed-loop system that does not produce waste. This integral solution involves taking ownership of the supply chain, manufacturing, and recycling process. Arshae's mission is to create beautiful products that inspire a new era of fashion where style and innovation are driven by inclusion, social well-being, and environmental health using advanced manufacturing technologies. In today's Industry 4.0 manufacturing environment, additive manufacturing is a very interesting and disruptive solution with unlimited potential for the footwear industry and seems to be a good alternative to achieve certain environmental goals. The footwear product that Arshae proposes and that is developed in the context of this study is part of a design approach for recyclability (DFS), assembly (DFA), and disassembly (DFD). This project aims to contribute to the circular manufacturing vision by focusing on the DFS, DFA and DFD design categories and bring technical solutions to the design of the product to facilitate its reintegration into a circular manufacturing loop.

The main objective of this study is therefore to facilitate manufactured shoe disassembly operations in order to increase the proportion of recycled shoes at the end of their life, which is currently only 5% in the world according to literature [6].

A. Background

Footwear manufacturing is a labor-intensive process, as a shoe usually consists of 65 pieces with about 360 manufacturing steps and a large part of the production process is still manual [7]. It takes a lot of machinery and skilled workers to make separate pieces and assemble them to create a finished pair of shoes. Footwear companies are looking for new ways to optimize the manufacturing process [8]. 3D printing offers a

promising alternative by allowing shoe companies to streamline the production of certain shoe components. However, such developments are still in their infancy and it is difficult to achieve a fully 3D printed shoe. To date, 3D printing is mainly used for the manufacture of the midsole - the shock-absorbing layer between the insole and the outsole. The mechanical performances are different from one material to another and have very distinct applications. However, the way parts are printed is critical to increase the capabilities of prototypes, as several process parameters, such as building orientation, printing speed, and layer thickness, affect mechanical properties [9].

B. *Presentation of the developed prototype*

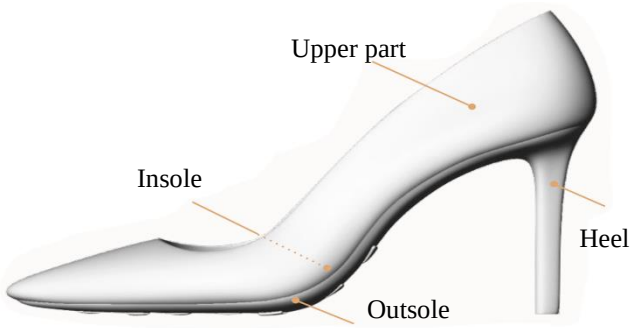

Figure 1. Illustration of the assembled high-heeled shoe after reduction of the number of parts

A high-heeled shoe is traditionally made up of more than 60 parts per pair. However, new production possibilities are appearing with the arrival of new manufacturing technologies, particularly 3D printing, with its various processes and technologies developed and improved each year. Hence, it becomes possible to design very complex parts and thus merge different assemblies into a monolithic part, which reduces the risk of defects due to assembly. The objective of the design proposed in this work is to unify some parts to maintain three (3) functional parts which will be called *Outsole*, *Insole* and *Upper part* as shown in figure 1. The outsole will be subject to the load distribution applied to the shoe due to the weight of the user and must therefore be able to withstand this user load with a well-defined safety factor. The insole shall have some flexibility and softness to provide comfort to the user while wearing the shoe. As well, the upper part - being in direct contact with the skin and having the role of containing the foot - will have to be elastic and rigid enough for the comfort of the shoe while keeping a certain resistance to tearing.

II. MATERIALS AND DESIGN

A. *Printing materials and technology*

Two 3D printing technologies are compared in this study - *Selective Laser Sintering (SLS)* and *Multi Jet Fusion (MJF)* - for simulations of resistance to static loads applied to the footwear during its use.

The materials deployed are “Polyamide 12 (Nylon12)” for the outsole, “HP 3D HR PA12” [10] for the MJF technology and “3DS DURAFORM PA” [11] for the SLS technique. A thermoplastic polyurethane (TPU) elastomer, “FS 1088A-TPU” from Farsoon Technologies, is selected for the upper part, which is printed by SLS technology.

B. *Design of the mechanical assembly system*

To achieve our objective, which is mainly focused on disassembly to complete recycling of the footwear at the end of its life, it is necessary to eliminate the use of chemical glue during the assembly process during production. Glue-less part connections greatly facilitate its disassembly to recycle parts made of different materials separately. This leads us to consider an exclusively mechanical assembly system instead of a chemical connection.

The proposed assembly system has been divided into two elements, the first part consists in designing an assembly system for the front part of the shoe, which is beyond the scope of this work, the second part consists of the development of a mechanical system for the rear part of the shoe (at the heel).

A Snapfit system is proposed to assemble the upper part and the outsole as shown in Figure 2. An aluminum pin (indicated in yellow in figure 2) has been introduced in the heel to increase the resistance to lateral impacts.

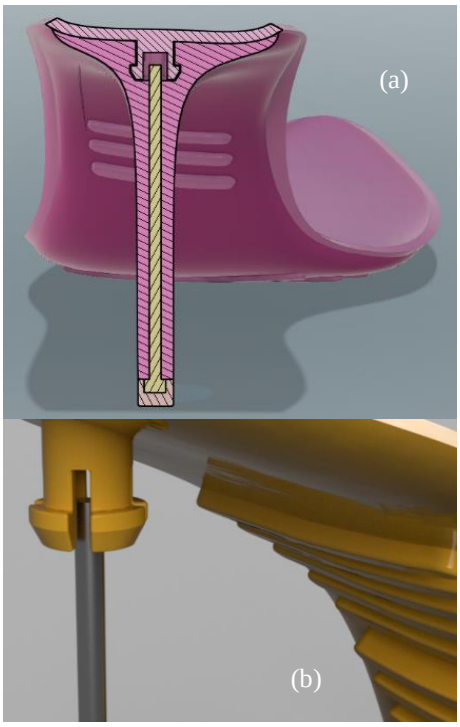

Figure 2. Cross section (a) illustrating the integration of the snapfit in the shoe, integration of the male part of the snapfit to the upper part (b)

III. THEORY

The snapfit was designed according to guidelines proposed by “The First Snap-Fit Handbook” written by Bonenberger [12]. An analytical calculation of the snapfit parameters such as the

assembly and disassembly force and the maximum bending of the rods was performed to validate the design.
The equations used in this section are based on dedicated work by Ticona [13] on snap fit joints in plastic parts. The maximum bending of each rod of the snapfit is calculated by

$$H_{max} = 0.555 \frac{l^2}{r} \frac{\varepsilon_{max}}{100} \quad (1)$$

where*:*
H_{max} is the maximum bending in mm.
l designates the length of the rods in mm.
r designates the external radius of the rods in mm.
ε_{max} designates the maximum allowable strain (this is recommended at 1/3 of the ultimate strain).

This gives us a maximum deflection of 8 mm to reach the allowable limits with a deformation of 1/3 of 340 % (maximum elongation provided by the manufacturer of the selected Farsoon FS1088A-TPU)[14].

To calculate the assembly force, the following equations were used:

$$F1 = \frac{3H\,E_S\,J}{l^3} \frac{\mu + \tan\alpha 1}{1 - \mu\,\tan\alpha 1} \quad (2)$$

$$J = 0.0508\,r^4 \quad (3)$$

With *H* the bending of the rods, *Es* the secant modulus of elasticity, *J* the moment of inertia, *l* the length of the rods, μ the coefficient of friction and $\alpha 1$ the angle of attack of the rods which is 30°.
The friction coefficient was estimated as μ = 0.329 after consulting the work on "Surface quality improvement of selective laser sintered polyamide 12" by Guo, Bai, Liu, and Wei [15] and the design guide cited above [12], which prescribes a friction coefficient μ between 0.3 and 0.4 for polyamide material.
Deploying equations (1), (2) and (3) gives us a force per rod equal to 6.24 N which must be multiplied by the number of rods, which is 4 in our case, giving us the assembly force of 24.96 N.
The disassembly force for an angle of 90° can be calculated with the following equation

$$F2 = A\,\tau_b \quad (4)$$

with *A* being the shear surface (Figure 3) of the rod and τb is 60% of the ultimate stress of the used material. This results in a disassembly force of 156 N per rod, which we multiply by 4 to have the total force, equalling to 624 N for the FS 1088A-TPU material, which is significantly higher than the resistance to normal forces applied for high heel pull-off as recommended by the footwear SATRA TM113:1996 standard (40Kgf).

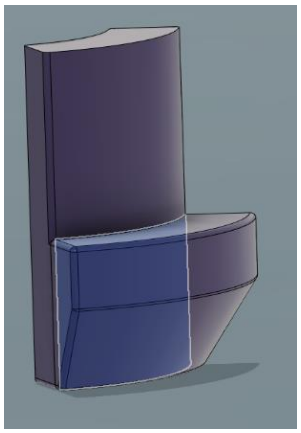

Figure 3. Illustration of the surface *A* used in equation (4) to calculate the disassembly force

IV. RESULTS AND DISCUSSION

A. Tensile Strength tests

Tensile tests were carried out to determine the main mechanical characteristics of each material (modulus of elasticity, ultimate strength, and ultimate elongation) and to implement them in a numerical simulation software to be able to compare the two materials. The tensile tests were performed following the ASTM D638-14 [16] protocol at a strain rate of 50 mm/minute on 7 specimens with an ambient temperature of 21°± 0.5. The average tensile strength test results are presented in Table 1.

Fig.4 and Fig.5 are presenting the results of the tensile strength measurements of these seven (7) samples printed respectively by MJF and SLS. It is observed from the graphs in Figure 2 that there is a clear difference between the two manufacturing processes in terms of ductility. In MJF the ultimate deformation is higher than in SLS, which is in good agreement with literature [17].This phenomenon can partially be explained by the relatively significant presence of micro porosity in SLS printed parts [18] and on the other hand the residues of the binding agent in MJF printed parts, which ensures better cohesion between the layers [19]. The obtained results are not far from the manufacturer's specifications [10, 11] in the respective data sheets of each material on each machine.

TABLE 1. Average uniaxial tensile tests results

Type	**Section (SD) [mm²]**		**Ultimate Strength (SD) [MPa]**		**Elongation (SD) [%]**		**Young Modulus (SD) [MPa]**		**Elastic Stress at 0.2% (SD) [MPa]**
	Sample	CAD	Sample	Supplier Data	Sample	Supplier Data	Sample	Supplier Data	Sample
SLS	41,91 (1.56)	39	41,71 (6.44)	43	4,81 (2)	14	1777,66 (96.67)	1586	32,44 (3,55)
MJF	40,43 (1.09)	39	49,41 (2,82)	50	14,92 (6)	17	1755,96 (114.21)	1900	30,28 (3,05)

(SD) = standard deviation

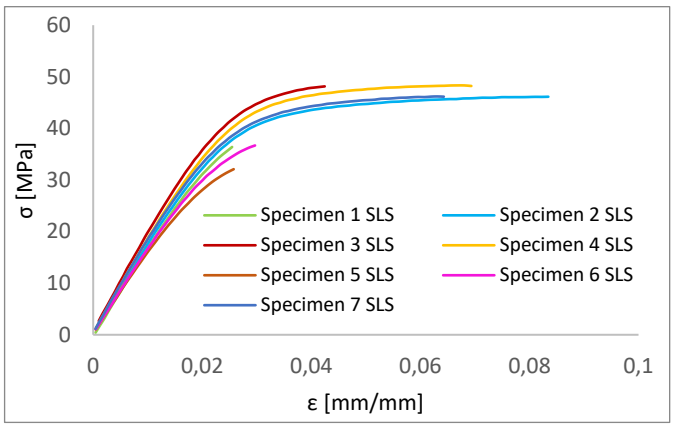

Figure 4. Tensile test stress/strain curves (SLS)

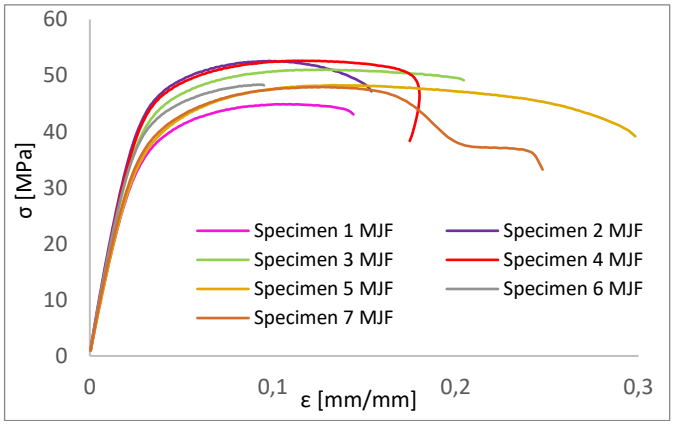

Figure 5. Tensile test stress/strain curves (MJF)

B. *Simulation of the snapfit assembly*

Fig.6 illustrates a mapping of the equivalent Von Mises stress in MPa on the male part of the TPU snapfit. We can clearly identify that the Von Mises stress reach a maximum of 17.57 MPa and it does not exceed the tensile strength of the FS 1088A-TPU, which is equal to 20 MPa according to the supplier.

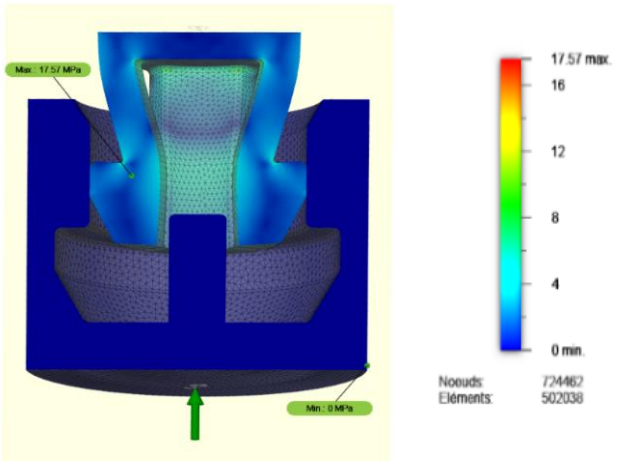

Figure 6. Von Mises stress distribution during snapfit assembly [MPa]

C. *Static study*

This section will focus on a static study (no evolution of the load as a function of time*) and* will be divided into 3 sub-sections, which will discuss respectively the plantar division which will be useful for the mapping of the load on the shoe, weight distribution, and stress of the shoe with the integration of the snapfit.

a) *Plantar division*

The soles of the feet are divided into 8 anatomical areas based on the work done by (Shang et al., 2020) [20], these areas are called (T1): big toe, (T2-5): smaller toes, (M1): first metatarsal, (M23): central forefoot, (M45): lateral forefoot, (MF): midfoot,(MH): medial heel, (LH): lateral heel. These areas are shown in Figure 7.

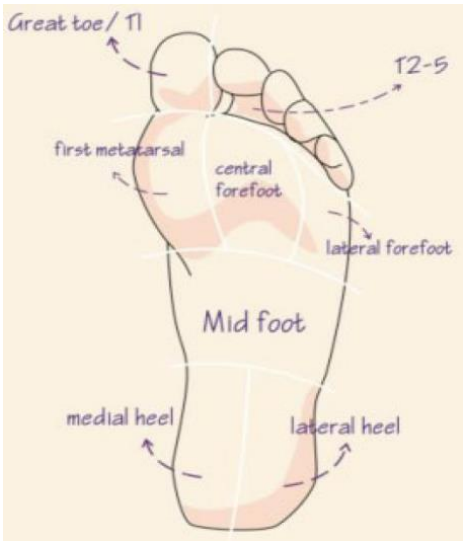

Figure 7. Diagram of plantar division, from [20]

b) *Weight distribution*

The weight distribution calculation is based on the experimental work of Shang et al.[20], which was conducted on about twenty adult female volunteers with a weight of (53.56 ± 5.75 kg) and an age of (20.89 ± 3.04 years) and which consists of measuring (using an F-Scan® measuring device from the manufacturer Tekscan® [21]) the distribution of forces applied to different types of footwear during their use. A static study was carried out by simulating the application of pressure on the different plantar areas described above according to the following table.

TABLE 2. Distribution of pressure on the assembled shoe

Contact Area	Surface [mm^2]	Pression [KPa]
T1	537	13,79
T2-5	796	10,6
M1	721	17,27
M23	662	18,09
M45	639	9,59
MF	626	6,09
MH	1285	10,42
ML	943	8,79

For reasons of simplification and calculation time, the upper part was cut at the height of the outer sole and a finite element analysis was performed, simulating the application of pressure on the different plantar areas described above, which is discussed in section IV. C. c).

c) Stressing of the shoe with the integration of the snapfit

The convergence rate of the intelligent mesh refinement is 3.01% after 9 iterations for the footwear, whose outsole is printed in MJF and 0.0045% after 5 iterations for the shoe whose outsole is printed in SLS.

As far as the safety factor in footwear is concerned, whether with the printed MJF or SLS outsole it is almost the same and it is higher than 6 which is a good result for footwear industry applications, based on footwear expert test findings. However, there is a small difference between the two types of printing on the total displacement at the midfoot (MF) with a displacement of 0.86 mm and 0.88 mm for the MJF and SLS respectively as shown in figure 8. The flexion of the midfoot can be limited by a metal piece called the shank. The integration of the snapfit does not create a weak zone despite the recess provided for its assembly, and this is due to the aluminum pin (inside the high heel) which plays a central role in absorbing the loads applied to the shoe.

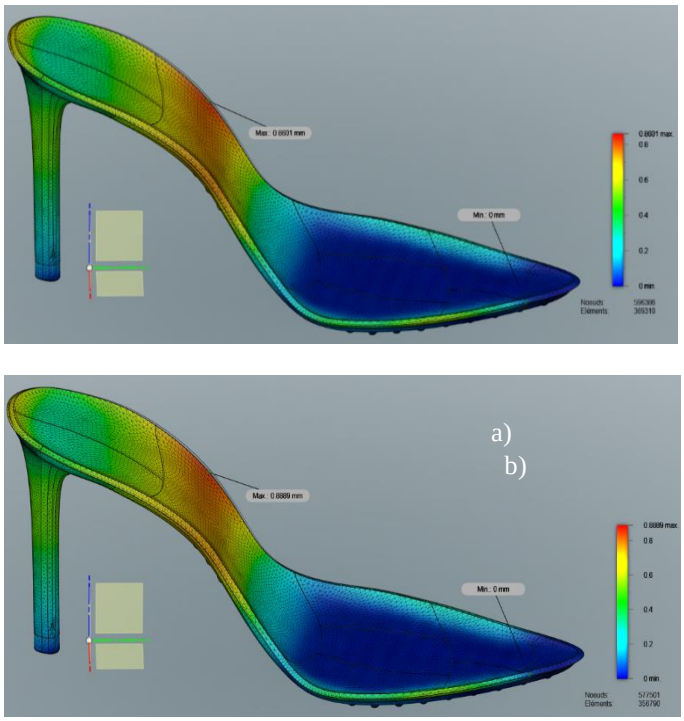

Figure 8. Mapping of the total displacement at any point of the shoe (a: MJF, b: SLS)

CONCLUSION

This paper focuses on a novel strategy to develop a line of fashionable footwear that responds to the business model trend of achieving circular manufacturing by recycling all its products and re-enter them in the production process to obtain a closed loop process. The research project consists in bringing technical solutions to the design of the product to facilitate its reintegration into such a circular manufacturing loop.

Based on the results of the simulations that have been carried out and the materials that have been selected, it is realistic to conclude that the model that has been developed with the pin is feasible and can resist with a safety factor of six (6) to the loading due to walking.

The assembly system proposed in this project solves the problem of assembling and disassembling the shoe for recycling purposes, e.g. by eliminating the need for (toxic) glues. It is also shown that the designed snapfit withstands a normal disassembly force of 624 N, which is high enough to keep the shoe well-assembled during use according to the footwear specific SATRA standards.

The obtained results support the main objective of this study, which is to facilitate disassembly operations to increase the proportion of recycled footwear and thus move towards circular manufacturing.

The recommendations that can be made from this conclusion are to validate the simulations that have been made and presented in this paper by mechanical tests and to carry out a study of material aging to determine the life span of the printed shoe.

ACKNOWLEDGEMENTS

The authors would like to acknowledge the financial support of Mathematics of Information Technology and Complex Systems (Mitacs) under grant IT20017.

REFERENCES

[1] WWF, "Biodiversity, biocapacity and better choices," in "Living Planet Report," ISBN 978-2-940443-37-6 2012. [Online]. Available: http://awsassets.panda.org/downloads/1_lpr_2012_online_full_size_single_pages_final_120516.pdf

[2] "Past Earth Overshoot Days." Earth Overshoot Day. https://www.overshootday.org/newsroom/past-earth-overshoot-days/ (accessed 07-01-2022.

[3] OCDE, *Material Resources, Productivity and the Environment*. 2015.

[4] R. Bleischwitz, P. Welfens, and Z. Zhang, "Sustainable Growth and Resource Productivity Economic and Global Policy Issues (ed. Bleischwitz," 01/01 2009.

[5] W. McDowall *et al.*, "Circular Economy Policies in China and Europe," *Journal of Industrial Ecology*, vol. 21, no. 3, pp. 651-661, 2017, doi: https://doi.org/10.1111/jiec.12597.

[6] M. J. Lee and S. Rahimifard, "An air-based automated material recycling system for postconsumer footwear products," *Resources, Conservation and Recycling*, vol. 69, pp. 90-99, 2012/12/01/ 2012, doi: https://doi.org/10.1016/j.resconrec.2012.09.008.

[7] L. Cheah *et al.*, "Manufacturing-focused emissions reductions in footwear production," *Journal of Cleaner Production*, vol. 44, pp. 18-29, 2013/04/01/ 2013, doi: https://doi.org/10.1016/j.jclepro.2012.11.037.

[8] C. F. S. Commitment, "Final Report," Global Fashion Agenda 2020.

[9] A. Pugalendhi, R. Ranganathan, and M. Chandrasekaran, "Effect of process parameters on mechanical properties of VeroBlue material and their optimal selection in PolyJet technology," *The International Journal of Advanced Manufacturing Technology*, vol. 108, no. 4, pp. 1049-1059, 2020/05/01 2020, doi: 10.1007/s00170-019-04782-z.

[10] HP. "HP 3D High Reusability PA 12." https://cimquest-inc.com/resource-center/HP/Materials/HP-PA12-Datasheet.pdf (accessed 05-02-2021.

[11] 3DSystem. "DURAFORM PA Plastic Datasheet." https://www.3dsystems.com/sites/default/files/2017-03/3D-Systems_DuraForm_PA_DATASHEET_USEN_2017.03.22_a_WEB.pdf (accessed 05-02-2021.

[12] P. R. Bonenberger, "The First Snap-Fit Handbook," in *The First Snap-Fit Handbook (Third Edition)*, P. R. Bonenberger Ed.: Hanser, 2016, pp. I-XXII.

[13] Ticona, "Design calculations for snap fit joints in plastic parts," in "Calculation. Design. Application. B.3.1," 2009.

[14] FARSOON. "Farsoon Polymer Materials." http://en.farsoon.com/downloadsfront.do?method=picker&flag=all&id=0c00cc87-7ac5-42e5-a5a5-72ea3c5e354a&fileId=46&isDownloadPermissions=true&memstate=/members_login.html (accessed 05-02-2021.

[15] J. Guo, J. Bai, K. Liu, and J. Wei, "Surface quality improvement of selective laser sintered polyamide 12 by precision grinding and magnetic field-assisted finishing," *Materials & Design*, vol. 138, pp. 39-45, 2018/01/15/ 2018, doi: https://doi.org/10.1016/j.matdes.2017.10.048.

[16] *Standard Test Method for Tensile Properties of Plastics D638*, ASTM, 2014.

[17] S. Rosso, R. Meneghello, L. Biasetto, L. Grigolato, G. Concheri, and G. Savio, "In-depth comparison of polyamide 12 parts manufactured by Multi Jet Fusion and Selective Laser Sintering," *Additive Manufacturing*, vol. 36, p. 101713, 2020/12/01/ 2020, doi: https://doi.org/10.1016/j.addma.2020.101713.

[18] B. Van Hooreweder, F. De Coninck, D. Moens, R. Boonen, and P. Sas, "Microstructural characterization of SLS-PA12 specimens under dynamic tension/compression excitation," *Polymer Testing*, vol. 29, no. 3, pp. 319-326, 2010/05/01/ 2010, doi: https://doi.org/10.1016/j.polymertesting.2009.12.006.

[19] F. Sillani, R. G. Kleijnen, M. Vetterli, M. Schmid, and K. Wegener, "Selective laser sintering and multi jet fusion: Process-induced modification of the raw materials and analyses of parts performance," *Additive Manufacturing*, vol. 27, pp. 32-41, 2019/05/01/ 2019, doi: https://doi.org/10.1016/j.addma.2019.02.004.

[20] J. Shang *et al.*, "Influence of high-heeled shoe parameters on biomechanical performance of young female adults during stair ascent motion," *Gait & Posture*, vol. 81, pp. 159-165, 2020/09/01/ 2020, doi: https://doi.org/10.1016/j.gaitpost.2020.07.065.

[21] Teskan. "Teskan F-Scan System." https://www.tekscan.com/products-solutions/systems/f-scan-system
(accessed 01-02-2021.